Kinematic Structure of a Heavy Rain Event from Dual-Doppler Radar Observations

SHAO Aimei [1] (邵爱梅), QIU Chongjian*[1] (邱崇践), and LIU Liping[2] (刘黎平)

[1] *Department of Atmospheric Sciences, Lanzhou University, Lanzhou* 730000

[2] *Chinese Academy of Meteorological Sciences, Beijing* 100081

(Received 25 June 2003; revised 24 December 2003)

ABSTRACT

The detailed kinematic structure of a heavy rain event that occurred in the middle reaches of the Yangtze River was investigated using dual-Doppler radar observation. A variational analysis method was developed to obtain the three-dimensional wind fields. Before the analysis, a data preprocessing procedure was carried out, in which the temporal variation with the scanning time interval and the effect of the earth curvature on the data position were taken into account. The analysis shows that a shear line in the lower and middle levels played an important role in the rainfall event. The precipitation fell mainly on the south end of the shear line where southerly flow prevailed and convergence and updraft were obvious. With the movement and decay of the shear line, the precipitation moved and decayed correspondingly.

Key words: heavy rain, mesoscale structure, dual-Doppler, variational method

1. Introduction

Heavy rain within the mei-yu front is the prime weather disaster in summer which occurs in the middle and lower reaches of the Yangtze River in China. The initiation and development processes associated with the phenomenon have been widely explored by means of synoptic-dynamic meteorology and numerical models by many scholars (e.g., Feng et al., 2001; Wang and Li, 2002; Chen, 1989; Zhao et al., 1998). However, for lack of necessary observations, the knowledge of the detailed kinematic and thermodynamic structure is still scarce, which also hampers our understanding of the physical mechanisms that initiate and maintain mesoscale heavy rain.

Doppler radar is currently the most powerful instrument for observing the structure of mesoscale systems and has been applied widely in mesoscale studies (e.g., Brandes, 1977; Ray et al., 1981; Carbone, 1983; Kessinger et al., 1987; Parsons and Kropfli, 1990; Atkins et al., 1995; Dowell and Bluestein, 1997). During the summers of 2001 and 2002, a field experiment called CHeRES (China Heavy Rain Experiment and Study) was performed to understand the physical processes of the heavy rain within the mei-yu front. In addition to routinely available synoptic data, multiple radar networks in the middle and lower reaches of the Yangtze River collected abundant observations. This provides the possibility for investigating the precise kinematic structure of the heavy rain occurring in this region.

In theory, the three-dimensional structure can be obtained by dual-Doppler observations in the precipitation area. However, because the observations of two radars differ in location and time and the vertical air component is determined basically by integrating the air mass continuity equation, in the classical compound technique (Testud and Chong, 1983) the raw data has to be interpolated to equally spaced grid points and iterative procedures are required to modify the vertical velocity. These procedures introduce errors and uncertainty into the analysis. Then a variational method can be used to unaffectedly combine the interpolation with the analysis procedures (especially since the interpolation is from equally spaced grid points onto observation locations) and can improve the analysis. So the method has been used even more in current dual-Doppler analysis.

In the present paper, a heavy rain event occurring in Hubei on 22 July 2002 was selected as the case

*E-mail: qiucj@lzu.edu.cn

study.

2. Analysis techniques

Dual-Doppler analysis is a general term for the process of constructing the wind field by using radial wind observations from two Doppler radars. The techniques have been developed since the late 1960s. Early dual-Doppler analyses stressed the synthesis of two independent Doppler velocity estimates in cylindrical (COPLAN) coordinates (e.g., Armijo, 1969; Lhermitte and Miller, 1970; Miller and Strauch, 1974). Subsequently, many dual-Doppler synthesized analyses were performed directly in the Cartesian system of coordinates instead of the COPLAN system (Brandes, 1977; Ray et al., 1980, 1981). Recently, variational methods that combine observations and physical constraints have been explored to retrieve 3D wind structures (Sun and Crook, 1997, 1998; Gao et al., 1999; Protat and Zawadzki, 1999, henceforth referred to as PZ99).

The aforementioned methods often suffer from notable difficulties, including the setting of vertical velocity boundary conditions, spatial interpolation errors, discretizations, uncertainties in radial wind estimates (due to sidelobes and ground clutter), and the nonsimultaneous nature of the measurements, These problems have been discussed in Miller and Strauch (1974), Ray et al. (1980), Gal-Chen (1982), Testud and Chong (1983), Chong et al. (1983a, b); Ziegler et al. (1983), and Shapiro and Mewes (1999). Moreover, since the microwave transmission curve is not straight and the earth's surface is not flat, the reliability of the dual-Doppler radar retrieval is questionable (Zhang et al., 2002).

The most pronounced difficulty is severe error accumulation in the vertical velocity when using the classical upward integration of the continuity equation. And this may affect the retrieval of the full 3D wind field. Therefore, many attempts have been proposed to improve the integration of the continuity equation. A recently proposed analysis technique for reducing vertical velocity errors comes from PZ99 and Gao et. al. (1999). PZ99 present an alternative to the constraining technique of Lateef (1967), O'Brien (1970), and Ray et al. (1980) for combating accumulating divergence errors. In this technique, the vertical velocity field at a given level is a linear combination of upward and downward integrations of the continuity equation. However, this technique requires the vertical velocity boundary conditions to be specified at both the top and bottom of the analysis domain. In particular, Gao et al. (1999) applied the anelastic mass conservation equation as a weak constraint, and the severe error accumulation in the vertical velocity was reduced because the explicit integration of the anelastic continuity equation is avoided.

In this paper, a technique based on a variational approach is used to retrieve the complete wind field. Before the processing of dual-Doppler analysis, a correction was performed to alleviate the errors associated with the nonsimultaneous nature of the measurements, the curvature of the earth, and the microwave transmission curve. The procedure proceeds as follows. First, the ranging of the radar observations is performed. Then, two successive volume scans of radar data are selected and the measurements are linearly interpolated to a single reference time. The processed data is then used as the input data for the dual-Doppler analysis.

The basic idea of the variational method is to adjust the analysis variables under some constraints so that the output variables match the observations as closely as possible. Now the wind components u, v, and $\tilde{w}$ in Cartesian coordinates are analysis variables. Here $\tilde{w} = w - w_{\rm t}$, where $w_{\rm t}$ is the terminal velocity of precipitation. Thus, we define a cost function as follows:

$$J(u,v,\tilde{w}) = \sum_m p_1 [R(u,v,\tilde{w}) - v_{r,\rm obs}]_m^2 + \sum_{i,j,k} p_2 C_{i,j,k}^2 + \sum_{i,j,k} p_3 S_{i,j,k}^2 + \sum_{i,j,k} p_4 B_{i,j,k}^2 \,. \quad (1)$$

Here p_i $(i = 1, 2, 3, 4)$ are the weightinged coefficients. The index m represents the observation point for both radars; i, j, and k represent grid point indexes in Cartesian coordinates; $v_{\rm r,\ obs}$ is the observed radial velocity; R stands for a function that maps the analysis variables (u, v, and $\tilde{w}$) from the analysis grid to the observed points. Here R has two components. The first component maps the analysis variables onto the data grid (m) by making a linear interpolation. The second component maps the analysis Cartesian velocity components onto the analysis radial velocity $v_{{\rm r},m}$, and is given by

$$v_{{\rm r},m} = \alpha_m u_m + \beta_m v_m + \gamma_m \tilde{w}_m \,, \quad (2)$$

where α_m, β_m, and γ_m are the direction cosines of the m th observation point, in the x, y, and z directions respectively, of the radar beam. Obviously the first term of the cost function represents the distance between the observed and analyzed radial velocity.

The second term of the cost function imposes a mass conservation equation constraint on the analyzed wind field. Here, we use

$$C = \frac{\partial u}{\partial x} + \frac{\partial v}{\partial y} + \frac{\partial w}{\partial z} - qw \,, \quad (3)$$

where $q = -\partial \ln p/\partial z$, and the value of q is 10^{-4} m^{-1} for the standard atmosphere. In the present paper, we have specified the value of w at the lower boundary, namely, $w_s = 0$.

The third term of the cost function is a smoothness constraint where S^2 is defined as follows:

$$S^2 = S_u^2 + S_v^2 + S_w^2 \,, \tag{4}$$

$$\begin{aligned} S_u^2 =&(u_{i+1,j,k} + u_{i-1,j,k} + u_{i,j+1,k} + u_{i,j-1,k} \\ &+ u_{i,j,k+1} + u_{i,j,k-1} - 6u_{i,j,k})^2 \,, \end{aligned} \tag{5}$$

The equations for S_v^2 and S_w^2 are similar to the equation for S_u^2. This smoothness term can reduce the effect of observational error on the analysis results.

The fourth term of the cost function is a background constraint and is defined as

$$\begin{aligned} B_{i,j,k}^2 =&(u_{i,j,k} - u_{i,j,k,\mathrm{b}})^2 + (v_{i,j,k} - v_{i,j,k,\mathrm{b}})^2 \\ &+ (\tilde{w}_{i,j,k} - \tilde{w}_{i,j,k,\mathrm{b}})^2 \,, \end{aligned} \tag{6}$$

where subscript b denotes the background field. To extend the region of the analysis field and reduce the observational error, three steps of analysis were carried out. First, a double grid interval is used in our analysis with no background ($p_4 = 0$). Then the original grid interval is used with the above results as the background field. Finally, some missing areas are filled by internal interpolation in the analysis field.

The problem is then to minimize the cost function J, and the quasi-Newton algorithm (Gilbert and Lemaréchal, 1989) is used to find the minimum. In our method, the iterative number of each analysis is 30, and the root-mean-square error (rms) between the analyzed velocity and observed velocity often reaches 1–2 m s^{-1}.

3. Data availability and analysis result

3.1 *Data availability*

A heavy rain occurred in the middle area of the Yangtze River on 22 July 2002, with which the associated synoptic situation was an upper trough and warm shear line in the middle and lower levels of the atmosphere. From 0800 LST 22 July to 0800 LST 23 July, six surface stations in Hubei Province reported more than 100 mm of rainfall. A dual-Doppler radar network also captured this mesoscale precipitation event.

One of the radars was an S-band Doppler radar located at Yichang (30.70°N, 111.29°E), and the other was a C-band Doppler radar located at Jingzhou (30.327°N, 112.192°E). The volume scanning mode for the Yichang radar consists of 14360 azimuth sweeps performed in ∼ 6 min, with an azimuthal resolution of 1.0° and gate spacing of 250 m/1000 m (velocity/reflectivity) over a maximum range of 230 km/460 km (velocity/reflectivity). The elevation angles are 0.5°, 1.5°, 2.4°, 3.4°, 4.3°, 5.3°, 6.19°, 7.5°, 8.69°, 10.0°, 12.0°, 14.0°, 16.7°, and 19.5°. The operation mode for the Jingzhou radar consists of a sequence of 14512 azimuth sweeps obtained in ∼ 6 min, with an azimuthal resolution of 0.7° and gate spacing of 300 m over a maximum range of 150 km. The Jingzhou radar, which has a Nyquist velocity of 12.4 m s^{-1}, was operated in coordination with the Yichang radar. The distance between the two radars was about 96 km. Figure 1 shows their locations in the observational area.

At 1108 LST 22 July 2002, precipitation moved over the dual-Doppler lobes. Two convective cells associated with this heavy rain appeared in the south of Yichang in the radar images (not shown). The cells moved from southwest to northeast. After three hours, the left reflectivity cell evolved into stratiformis, while the right one evolved into a convective cloud band. In this case, a posterior convective cloud played a major role in the intensification of the right cell. At the moment, this cell became weak and gradually moved out of the observational area.

To provide a better insight into the three-dimensional airflow structure of this system in the limited dual-Doppler coverage area, we examine the evolutive process of a strong reflectivity in southeast Yichang (the right cell). A square domain was selected as our analysis area (shaded part in Fig. 1). The grid is 41×41 × 21 points with the origin 10 km east and 120 km south of the Yichang radar site, and the grid interval is 2000 m in the horizontal and 500 m in the vertical.

3.2 *Data resolution analysis*

To show the accuracy of the analysis result, the resolution of the radar observations is analyzed. As

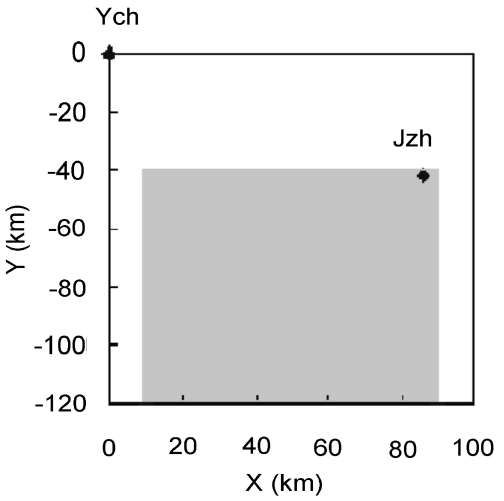

Fig. 1. The locations of the radars and the retrieval domain (shaded). Ych is Yichang and Jzh is Jingzhou.

Table 1. The averaged vertical resolution (AVR) at some given levels (units: m).

Altitude	500	1500	2500	3500	5500	4500	6500	7500	8500
AVR	759.31	1338.75	1300.61	1291.05	1377.50	1328.53	1420.57	1473.82	1567.40

described in the previous section, the radial resolution is 250 m or 300 m. In the dual-Doppler analysis domain, the radial distance between the radar site and the observed points reaches a peak of 150 km, and the tangential resolution comes to a climax of 2618 m with an azimuthal resolution of 1.0°. In most of the analysis gridpoints, the tangential resolutions of the two radars are within the horizontal grid interval (2 km). This indicates that the horizontal resolution of the radar measurements is quite high.

However, since one volume scan of a radar measurement only includes 14 elevation angles and its uneven compart, the averaged vertical resolution in the analysis levels decreases with altitude (see Table 1) and it is over 1000 m at most levels. The above analysis indicates that the refined vertical structure of a mesoscale system may not be completely covered by using the radar data, though data gaps can be filled by the smoothness constraint in the cost function.

3.3 *Result analysis*

First, a series of horizontal sections of 3D wind fields and reflectivity are presented in Fig. 2 in order to illustrate the major changes of the heavy rain structure and flow characteristics. One can see that the change of the three-dimensional structure of the wind fields is not obvious in our analysis area from 1136 to 1236 LST. In the middle and low levels, a southwest-northeast direction shear line, which was formed by the confluence of the weaker easterly airflow and a stronger southerly inflow, emerged in our analysis domain and moved slowly to the northeast. During the period, this system was in a developing stage. The precipitation mainly occurred at the rear of the shear line where the southerly flow prevailed and strengthened with time. A vertical cross section of wind fields at 1236 LST (Fig. 3a) also shows that updraft was stronger in the area where southerly airflow occurred, and reached a peak within the high reflectivity area. Aloft, southwesterly flow was predominant and expanded gradually to the north.

During the period between 1108 and 1300 LST, the reflectivity also took on an intensifying trend. As we can see from Fig. 2a and Fig. 2c, the reflectivity field was stronger at 1236 LST than an hour previously, with values in excess of 40 dBZ. This strong reflectivity signature is linked to intensification of the updraft. The primary reason for this was the formation of a back-building reflectivity. About at 1119 LST, this back-building reflectivity emerged in the southeastern part of the analysis domain, and rapidly developed and achieved maturity at about 1300 LST. It led to the development of the origin reflectivity cell and an increase in local precipitation. The precipitation pattern observed at the surface stations also reflected this signature. For instance, the precipitation rate increased from 5.9 mm h^{-1} at 1200 LST to 18.5 mm h^{-1} at 1300 LST in Gongan, Hubei. Moreover, it is evident that the movement of the reflectivity field was consistent with the movement of the shear line.

After 1400 LST, the reflectivity had become weaker and moved out of the analysis domain gradually. At this time, the system was in the decaying stage. At a 2-km altitude, the southerly inflow had become southwesterly flow at the rear of the shear line at 1447 LST (Fig. 2e). The precipitation also weakened. A uniform southwesterly predominated at a 5-km altitude (Fig. 2f). And updraft became weaker in the south of the analysis area (Fig. 3b). The vertical cross section also indicates that the vertical vortex in the north of the analysis domain was weaker than before.

Further, Fig. 4 and Fig. 5 give horizontal sections of the divergence field and vorticity field at 1236 LST, respectively. Convergence and a positive vorticity signature appeared in the strong reflectivity area at a 2-km altitude. Aloft, divergence can be found in the strong reflectivity area at the 5-km level.

The above analysis indicates that the change of southerly flow played an important role in this rainfall event, which was closely linked to the development of the system. In this mesoscale system, the location of the mesoscale shear line was consistent with the locations of the high reflectivity area, convergence, and positive vorticity. In this case, a "back-building" reflectivity come easily into being behind the original reflectivity band. The emergence of back-building is the reason for the increase in the rainfall.

4. Conclusions

A variational method of synthesizing the three-dimensional wind field from dual-Doppler radar observations is presented and applied to study the kinematic structure of a heavy rain event herein. The analysis indicated that a southwest-northeast-oriented shear line

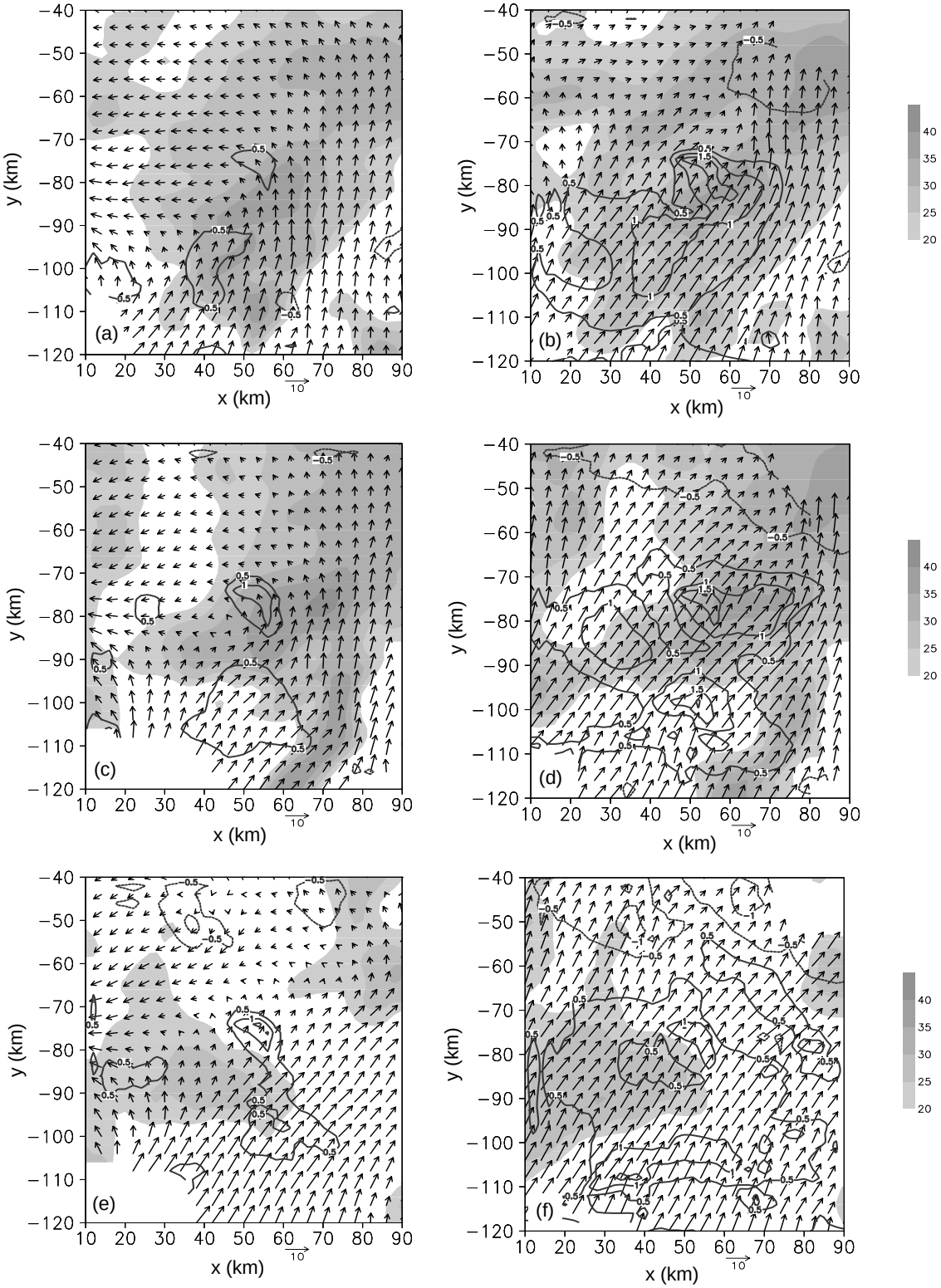

Fig. 2. Horizontal cross sections of airflow (arrows), vertical wind component (contours every 0.5 m s^{-1}) and reflectivity (shaded) at (a) 2-km altitude at 1136 LST; (b) 5-km altitude at 1136 LST; (c) 2-km altitude at 1236 LST; (d) 5-km altitude at 1236 LST; (e) 2-km altitude at 1447 LST; (f) 5-km altitude at 1447 LST 22 July 2002.

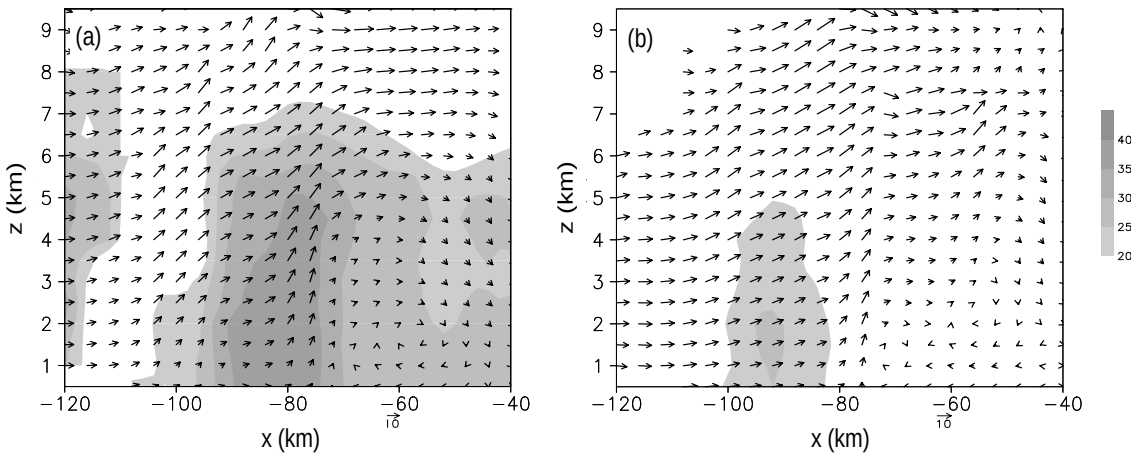

Fig. 3. Vertical cross section of airflow and reflectivity (shaded) at $x = 60$ km at (a) 1236 LST, (b) 1447 LST (vertical velocity is magnified 5 times).

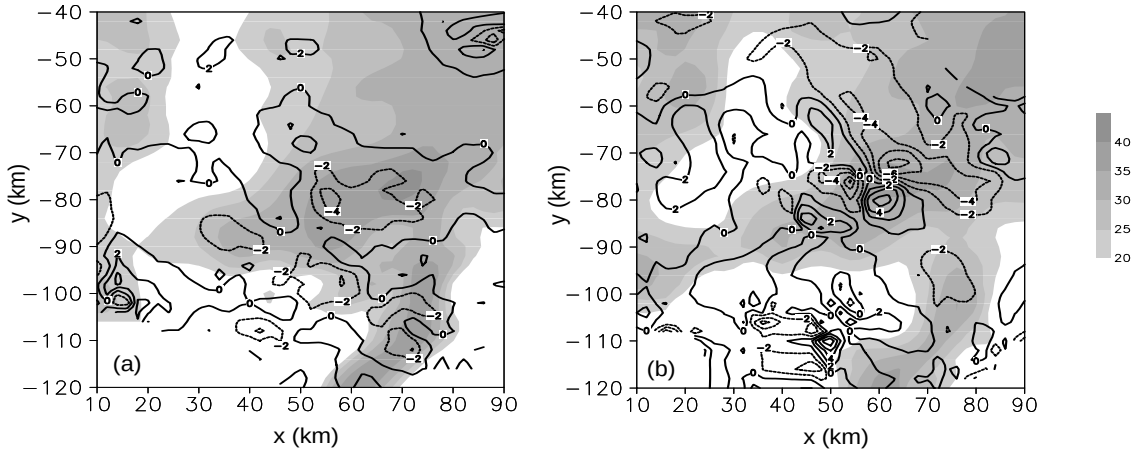

Fig. 4. The divergence (contours) and reflectivity (shaded) at (a) 2-km altitude, (b) 5-km altitude at 1236 LST. Contours are displayed every 2×10^{-4} s^{-1}.

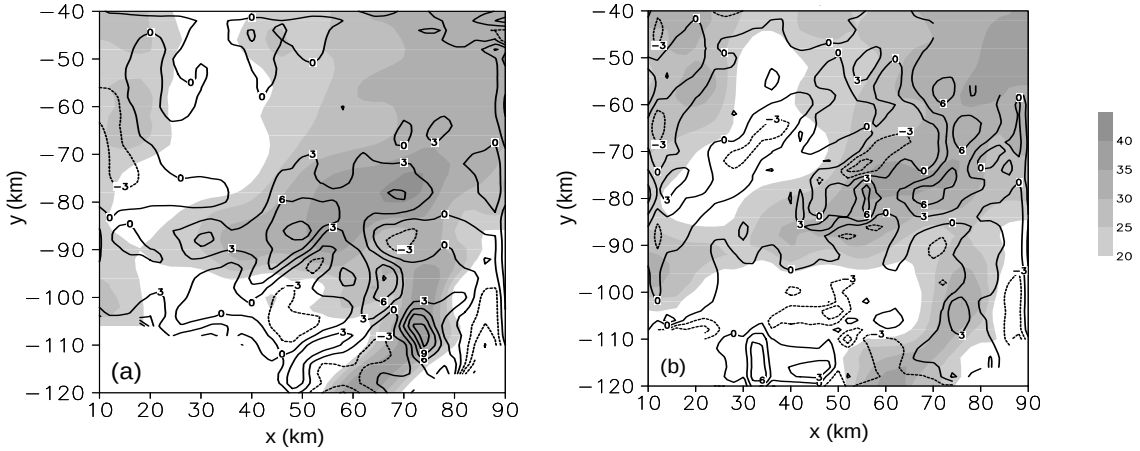

Fig. 5. Vorticity (contours) and reflectivity (shaded) at (a) 2-km altitude, (b) 5-km altitude at 1236 LST. Contours are displayed every $3{\times}10^{-4}$ s^{-1}.

in the lower and middle levels, which was formed by weaker easterly airflow and southerly flow, played an important role in this rainfall event. The precipitation occurred in the area where the southerly wind prevailed and where convergence and updrafts were obvious. With the movement and development of the shear line, the precipitation field moved correspondingly. In the developing stage of this system, the emergence and merging of a back-building reflectivity resulted in the intensification of this rainfall system and an increase in precipitation as reported by the surface stations.

It was noted that the horizontal scale of heavy rains within the mei-yu front, as different from a supercell storm, is relatively large, therefore the limited dual-Doppler coverage area impedes our ability to view a panorama of the system. The lower vertical resolution of the radar observations also influences also our analysis for the detailed vertical structure of the system. Perhaps combining dual-Doppler analysis with the retrieval technique from single radar will be an effectiveual approach to partly overcome this defect. Thus, it is a topic of future work.

Acknowledgments. This work was supported by the National Natural Science Foundation of China (Grant No. 40175010)

REFERENCES

Armijo, L., 1969: A theory for the determination of wind and precipitation velocities with Doppler radars. *J. Amos. Sci.*, **26**, 570–573.

Atkins, N. T., T. M. Weckwerth, and R. M. Wakimoto, 1995: Observations of the sea-breeze front during CaPE. Part II: Dual-Doppler and aircraft analysis. *Mon. Wea. Rev.*, **123**, 944–969.

Brandes, E. A., 1977: Flow in severe thunderstorms observed by dual-Doppler radar. *Mon. Wea. Rev.*, **105**, 113–120.

Carbone, R. E., 1983: A severe frontal rainband. Part II: Tornado parent vortex circulation. *J. Amos. Sci.*, **40**, 2639–2654.

Chen Shoujun, 1989: The vertical coupling of upper and lower jets in a heavy rainfall case during the late period of mei-yu season—numerical experiments.*Acta Meteorologica Sinica*, **47**(1), 8–16. (in Chinese).

Chong, M., J. Testud, and F. Roux, 1983a: Three-dimensional wind field analysis from dual-Doppler radar data. Part II: Minimizing the error due to temporal variation. *J. Climate Appl. Meteor.*, **22**, 1216–1226.

Chong, M., J. Testud, and F. Roux, 1983b: Three-dimensional wind field analysis from dual-Doppler radar data. Part III: The boundary condition: An optimum determination based on a variational concept. *J. Climate Appl. Meteor.*, **22**, 1227–1241.

Dowell, D. C., and H. B. Bluestein, 1997: The Arcadia, Oklahoma, storm of 17 May 1981: Analysis of a supercell during tornadogenesis. *Mon. Wea. Rev.*, **125**, 2562–2582.

Feng Wuhu, Cheng Linsheng, and Cheng Minghu, 2001: Nonhydrostatic numerical simulation for the "96·8" extraordinary heavy rainfall and the developing structure of mesoscale system. *Acta Meteorologica Sinica*, **59**(3), 294–307. (in Chinese)

Gal-Chen, T., 1982, Errors in fixed and moving frame of references: Applications for convectional and Doppler radar analysis. *J. Atmos. Sci.*, **39**, 2279–2300.

Gao，J. D., M. Xue, A. Shapiro, and K. K. Droegemeier, 1999: A variational method for the analysis of three-dimensional wind fields from two Doppler radars. *Mon. Wea. Rev.*, **127**, 2128–2142.

Gilbert, J. C, C. Lemaréchal, 1989: Some numerical experiments with variable storage quasi-Newton algorithms. *Math Programming*, **45**, 407–435.

Kessinger, C. J., P. S. Ray, and C. E. Hane, 1987: The Oklahoma squall line of 19 May 1977. Part I: A multiple Doppler analysis of convective and stratiform structure. *J. Atmos. Sci.*, **44**, 2840–2864.

Lateef, M. A., 1967: Vertical motion, divergence, and vorticity in the troposphere over the Caribbean, August 3–5, 1963. *Mon. Wea. Rev.*, **95**, 778–790.

Lhermitte, R. M., and L. J. Miller, 1970: Doppler radar methodology for the observation of convection storms. Preprints, *14th Conf. On Radar Meterology*, Tucson, AZ, Amer. Meteor. Soc., 133–138.

Miller, L. J., and R. G. Strauch, 1974: A dual Doppler radar method for the determination of wind velocities within precipitating weather systems. *Remote Sens. Environ.*, **3**, 219–235.

O'Brien, J. J., 1970: Alternative solutions to the classical vertical velocity problem. *J. Appl. Meteor.*, **9**, 197–203.

Protat, A., and I. Zawadzki, 1999: A variational method for real-time retrieval of three-dimensional wind field from multiple-Doppler bistatic radar network data. *J. Atmos. Oceanic. Technol.*, **16**, 432–449.

Parsons, D. B., and R. A. Kropfli, 1990: Dynamics and fine structure of a microburst. *J. Appl. Meteor.*, **9**, 197–203.

Ray, P. S., R. J. Doviak, G. B. Walker, D. Sirmans, J. Carter, and B. Bumgarner, 1975: Dual-Doppler observations of a tornadic storm. *J. Appl. Meteor.*, **14**, 1421–1530.

Ray, P. S., C. L. Ziegler, W. Bumgarner, and R. J. Serafin, 1980: Single- and multiple-Doppler radar observations of tornadic storms. *Mon. Wea. Rev.*, **108**, 1607–1625.

Ray, P. S., B. C. Johnson, K. W. Johnson, J. S. Bradberry, J. J. Stephens, K. K. Wagner, R. B. Wilhelmson, and J. B. Klemp, 1981: The morphology of several tornadic storms on 20 May 1977. *J. Atmos. Sci.*, **38,** 1643–1663.

Shapiro, A., and J. J. Mewes, 1999: New formulations of dual-Doppler wind analysis. *J. Atmos. Oceanic Technol.*, **16**, 782–792.

Sun, J., and N. A. Crook, 1997: Dynamical and microphysical retrieval from Doppler radar observations using a cloud model and its adjoint. Part I: Model development and simulated data experiments. *J. Atmos. Sci.*, **54**, 1642–1661.

Sun, J., and N. A. Crook, 1998: Dynamical and microphysical retrieval from Doppler radar observations using a cloud model and its adjoint. Part II: Retrieval experiments of an observed Florida convective storm. *J. Atmos. Sci.*, **55**, 835–852.

Testud, J. D., and M. Chong, 1983: Three-dimensional wind field analysis from dual-Doppler radar data. Part I: Filtering, interpolation and differentiating the raw data. *J. Climate Appl. Meteor.*, **22**, 1204–1215.

Wang Jianjie, and Li Zechun, 2002: Numerical simulation and diagnostic analysis on mesoscale convective systems of a torrential rain case in mei-yu period of 1998. *Acta Meteorologica Sinica*, **60**(2), 146–155. (in Chinese)

Zhang Peiyuan, Zhou Haiguang, and Hu Shaoping, 2002: Reliability study of determining wind with dual-Doppler radars. *Journal of Applied Meteorology Science*, **13**, 485–496. (in Chinese)

Ziegler, C. L., P. S. Ray, and N. C. Knight, 1983: Hail growth in an Oklahoma multicell storm. *J. Atmos. Sci.*, **40**, 1768–1791.

Zhao Sixiong, Sun Jianhua, Chen Hong, and Zhang Feng, 1998: Study of Heavy Rainfall in the Changjiang River during July 1998. *Climatic and Environmental Research*, **3**(4), 368–381. (in Chinese)